

## Micro shape and rough surface analysis by fringe projection

Klaus Leonhardt, Ulrich Droste, Stefan Schön, Christoph Volland, and Hans J. Tiziani  
 Institut fuer Technische Optik, Universitaet Stuttgart  
 Pfaffenwaldring 9, 7000 Stuttgart 80, Germany

### ABSTRACT

A new microscopic fringe projection system is described. Projection of the grating and imaging of the fringes is accomplished by the same objective. The spectrum of the binary grating is spatially filtered and projected into the aperture with a lateral shift. This leads to telecentric projection and imaging under oblique incidence. Topographies of specularly as well as diffusely reflecting surfaces can be obtained. The measurement of rough, technical surfaces is demonstrated.

### 1. PRINCIPLE OF FRINGE PROJECTION

By conventional fringe projection only diffusely reflecting objects can be measured, because the optical axis of the imaging system is normal to the mean tangential plane of the object and forms an angle  $\beta$  with respect to the axis of the projection system. We describe a symmetric configuration with  $\pm \beta$  for the directions of projection and imaging through the same high aperture objective MO, Fig.1. In this way, regular reflection is included and an optimum range of scattering angles allows for micro shape measurements on smooth surfaces as well as for roughness measurements on critical surfaces.

By spatial filtering, only the  $-1, 0$  and  $+1$  orders of the spectrum are transmitted (Fig. 2). The spectrum is shifted off-axis by the distance  $d$ , so that the principal rays form an angle  $\beta$  with the optical axis in the object space. As the pupil of the microscope objective is not accessible, filtering is done in plane F, conjugate to the pupil EP. Thus projection and imaging are both telecentric. The intensity  $I(x,Y)$  perpendicular to the projected lines is:

$$I(x,Y) = I_0(1 + 2 s^2 + 4 s \cos \alpha + 2 s^2 \cos 2\alpha), \quad (1)$$

$$\alpha(x) = \frac{2\pi}{p} (x + 2 h(x) \sin \beta), \quad (2)$$

where  $h(x)$  is the topography height,  $s = \text{sinc}(0.5) = 0.637$ ,  $p =$  grating period, and  $\beta$  the projection angle. The height variation  $\Delta h$  due to a local fringe displacement  $\Delta x$  in  $x$ -direction is:

$$\Delta h = \frac{\Delta x}{2 s \sin \beta}, \quad \sin \beta = \frac{d}{f_{MO}}, \quad (3)$$

where  $f_{MO}$  is the focal length of MO. One of our phase algorithms is a spatially integrating synchronous detection. Due to the spatial filtering, the fringe intensity Eq.(1) is composed of the cosine of the fundamental order and of a second order contribution, only. Therefore, we alternatively can apply a phase step algorithm which is insensitive to this second order contribution.

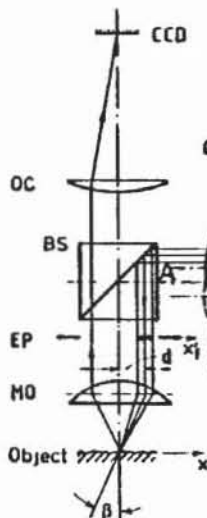


Fig.1

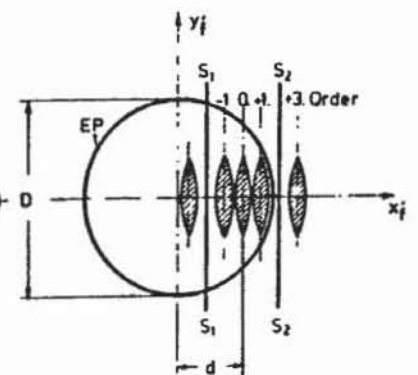


Fig.2

## 2. OPTICAL AND DIGITAL PROCESSING AND RESOLUTION

In order to prevent topography errors as spikes and ripples we apply a number of optical and digital processing steps. Temporal noise of different camera frames is statistically independent and can be suppressed by averaging several intensity frames. Spatial noise is more difficult. Additive noise and the second order contribution of the intensity Eq.(1) can be eliminated by subtraction of a  $\pi$ -shifted intensity. However multiplicative noise and variations of the illuminating intensity and of the surface reflexivity are not compensated. We found that for topographies of very rough surfaces, a division by a  $\pi$ -shifted second frame of the intensity field results in less spikes and less unwrapping errors. Furthermore, parts of the surface with large local slopes or discontinuities may lead to shadowing. In this case, we average the height from a first direction with the unshadowed height field of a second frame under the opposite direction, by shifting the spectrum of the grating to the opposite border of the pupil EP with lens  $O_1$ . Finally, due to residual optical aberrations, the images of the projected grating lines deviate from perfect straight lines. The topography even of a perfect plane can be deformed. To compensate this, we subtract the topography of a good plane mirror from each topography.

So far, lateral resolution is determined by the sample distance. Vertical resolution  $\delta_h$  (rms of the topography noise) is limited by noise:

$$\delta_h = \frac{p}{4 \pi \sin \beta S \sqrt{N}}, \quad (4)$$

where  $p$  is the period of the projected grating on the object,  $\beta$  is the projection angle and  $N$  is number of sample values within one period.  $S$  is the signal to noise ratio of the intensity signal, and can be assessed experimentally from a trace of the camera intensity across the grating lines.

## 3. APPLICATIONS

Fig.3 shows a topography of the largest groove of a PTB calibration standard for stylus instruments. The object field is  $531 \mu\text{m} \times 531 \mu\text{m}$ . The certified depth is  $9.00 \mu\text{m} \pm 0.05 \mu\text{m}$ , and the theoretical height resolution according to Eq.(4) is  $\delta_h = 162 \text{ nm}$ . Both theoretical values agree well with measurements. The topography of Fig.4 is a detail of a micro lithography. A  $20 \times 0.5$  objective was used and several intensity fields have been averaged. The object field is  $380 \mu\text{m} \times 380 \mu\text{m}$  and the vertical resolution is  $\delta_h \approx 25 \text{ nm}$ .

Fringe projecting microscopy, FPM, is a powerful tool for surface analysis. It is much more robust than interference microscopy. It can be adapted for rough, machined surfaces. This is a main field for future applications. On the other hand, for smooth surfaces and high aperture objectives, vertical resolution can be a few nm.

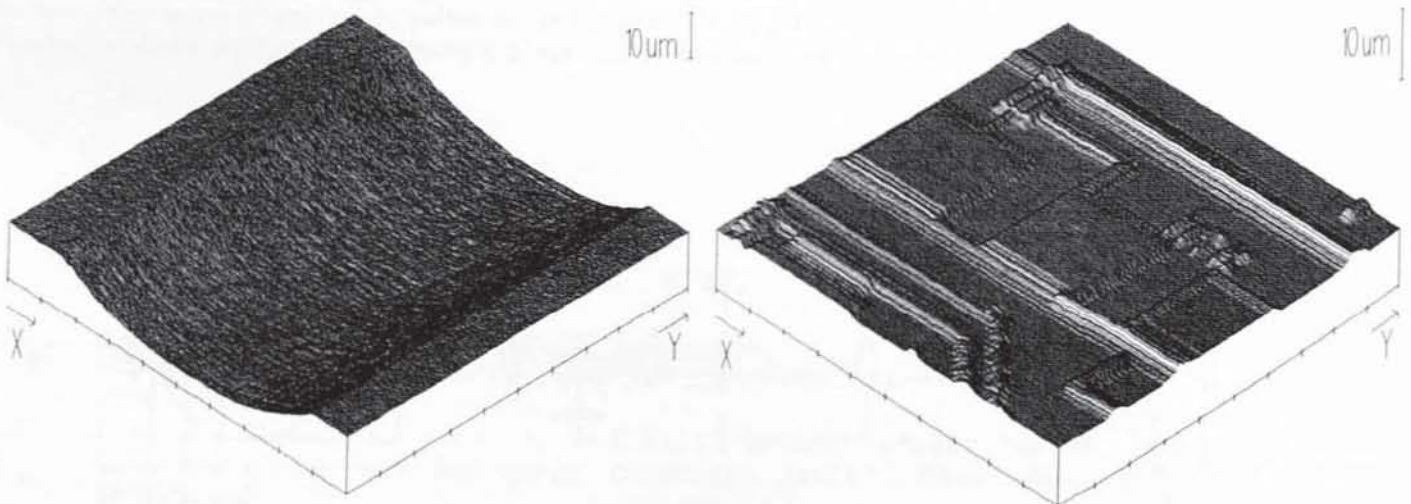


Fig.3

Fig.4